Computer Modeling of the Equilibrium Position Magnetization Precession in the Ferrite Plate

V. S. Vlasov[1] [a], D. A. Suslov[2] [b], V. G. Shavrov[2] [c] and V. I. Shcheglov[2]

[1] *Syktyvkar State University, Syktyvkar, Russia*

[2] *Kotel'nikov Institute of Radio Engineering and Electronics, Russian Academy of Sciences, Moscow, Russia*

Keywords: Nonlinear Magnetization Precession, Computer Modelling, Ferrite Plate.

Abstract: Nonlinear equilibrium position magnetization precession in a normally magnetized ferrite plate is modeled in the Matlab system. The magnetization motion equations for 3 cases are given: the isotropic plate, the plate with uniaxial anisotropy and the plate with cubic anisotropy. Differential equation system for magnetization vector relative to magnetization components is solved by Runge-Kutta method in the Matlab. The code of the program for modeling the magnetization dynamics is given. The program allows to build parametric portraits of the magnetization and study their features under various types of the plate anisotropy. The features of parametric portraits for these three cases of the anisotropy are considered.

1 INTRODUCTION

There is the great interest in modeling the dynamics of nonlinear magnetic systems (Vlasov et al., 2022; Vlasov et al., 2020). It is caused by promising applications of magnetic nanostructures in spintronics and nanoelectronics (Shelukhin et al., 2022; Barman et al., 2020). Computer modeling is also relevant due to the impossibility of analytical solution of the magnetization dynamics nonlinear problems (Shavrov and Shcheglov, 2021). One of the interesting types of the magnetization vector precession in planar structures is the equilibrium position precession. Such precession can be observed in the perpendicular magnetized plate (Shavrov and Shcheglov, 2021). In this case, the DC field is smaller than the demagnetization field and the magnetization vector is deviated from the direction of the field in the equilibrium state. When the alternating field is turned on, the precession of the magnetization vector appears relative to the equilibrium position. Moreover, the equilibrium position moves along the "big circle" of the precession portrait and we see the rings filled the "big circle". So, the realization of "precession in precession" is obtained (Shavrov and Shcheglov, 2021; Vlasov et al., 2011).

The magnetization dynamics for the equilibrium position precession cannot be found by using analytical formulas. Therefore, the only theoretical way to study the equilibrium position precession is the computer modeling using numerical solution methods (Shavrov and Shcheglov, 2021; Vlasov et al., 2012; Vlasov et al., 2013). Matlab package solution methods are used to simulate the motion of the magnetization vector in the present paper.

The paper is devoted to modeling the equilibrium position precession with the symmetric and asymmetric DC fields orientation in the isotropic ferrite plate and for cases of the uniaxial and cubic anisotropy (Shavrov and Shcheglov, 2021).

2 GEOMETRY AND BASIC EQUATIONS

2.1 Geometry of the Problem

Let's consider the normally magnetized ferrite plate. The 3 cases of equilibrium position precession for different types of the plate anisotropy are studied: 1. the isotropic plate; 2. the plate with uniaxial

[a] https://orcid.org/0000-0001-6902-608X
[b] https://orcid.org/0000-0002-1962-1195
[c] https://orcid.org/0000-0003-0873-081X

Vlasov, V., Suslov, D., Shavrov, V. and Shcheglov, V.
Computer Modeling of the Equilibrium Position Magnetization Precession in the Ferrite Plate.
DOI: 10.5220/0011906700003612
In *Proceedings of the 3rd International Symposium on Automation, Information and Computing (ISAIC 2022)*, pages 115-120
ISBN: 978-989-758-622-4; ISSN: 2975-9463

anisotropy; 3. the plate with cubic magnetic anisotropy. The general geometry of the problem is illustrated in Figure 1. Figure 1a shows the plate with uniaxial anisotropy. Figure 1b illustrates the plate with cubic anisotropy. The ferrite plate is magnetized by the DC field perpendicular to its plane, the alternating field is applied in the plane of the plate. The xOy plane of the Cartesian coordinate system Oxyz coincides with the plane of the plate. The z axis is perpendicular to the plate plane. For the case of the isotropic ferrite plate, the DC field may also have weak components in the plane of the plate.

Firstly, let us consider in detail the geometry of the problem for the ferrite plate with uniaxial magnetic anisotropy (Shavrov and Shcheglov, 2021). The easy axis (EA) is deviated from the normal to the plate plane by the arbitrary angle. Such geometry of the problem is shown in Figure 1a. The direction of the EA is given by 2 angles in the spherical coordinate system θ_a, φ_a.

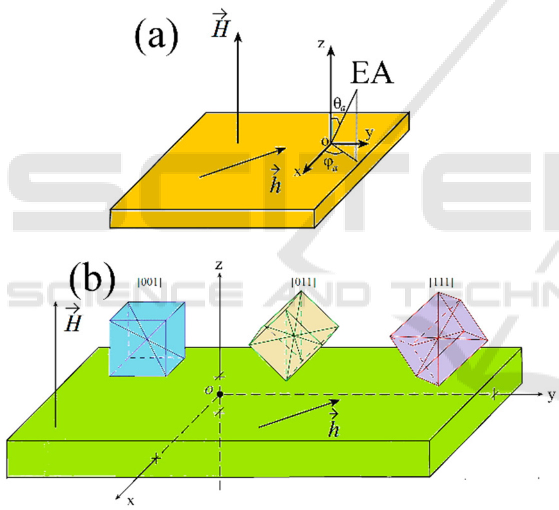

Figure 1. Geometry of the problem.

For the case of the plate with cubic anisotropy, three variants of the orientation of the cubic crystallographic cell are considered in Figure 1b:
1) ORIENTATION [001]: one of the crystallographic axes of the type [001] which is the edge of the cube is directed along the normal from the plate plane;
2) ORIENTATION [011]: one of the axes of the type [011] is directed along the normal from the plate plane, i.e. the diagonal of the cube face;
3) ORIENTATION [111]: one of the axes of type [111], i.e. the spatial diagonal of the cube, is directed along the normal from the plane of the plate (Vlasov et al., 2013).

2.2 Basic Equations

The problem of the magnetization vector dynamic behavior is solved in the coordinate system associated with the DC field, i.e. Oxyz. The expressions for the energy and the uniaxial anisotropy field for the case of the easy axis rotated by angles θ_a, φ_a are obtained in the work (Shavrov and Shcheglov, 2021). The expressions for the energy and fields of the cubic anisotropy, for orientations [001], [011], [111] are obtained similarly in work (Vlasov et al., 2013).

We further assume that the DC field $\vec{H}$ is not sufficient to align the magnetization vector in the equilibrium state perpendicular to the plane of the plate. The components of the alternating field have the form:

$$h_x = h_0 \sin(2\pi F t),\ h_y = -h_0 \cos(2\pi F t) \quad (1)$$

where F – the alternating field frequency, h_0 – its amplitude.

The magnetization equilibrium position precession is possible to observe for such magnetic fields orientation relative to the plate plane, in certain circumstances. This precession type is the equilibrium position motion around the direction of the DC field with the frequency significantly lower than alternating field frequency.

To solve the problem of the magnetization vector dynamic behavior we use the Landau–Lifshitz magnetization motion equations with the dissipative Gilbert term (LLG) (Shavrov and Shcheglov, 2021):

$$\frac{\partial m_x}{\partial t} = -\frac{\gamma}{1+\alpha^2}\left[\left(m_y + \alpha m_x m_z\right)H_{ez} - \left(m_z - \alpha m_y m_x\right)H_{ey} - \alpha\left(m_y^2 + m_z^2\right)H_{ex}\right], \quad (2)$$

$$\frac{\partial m_y}{\partial t} = -\frac{\gamma}{1+\alpha^2}\left[\left(m_z + \alpha m_y m_x\right)H_{ex} - \left(m_x - \alpha m_z m_y\right)H_{ez} - \alpha\left(m_z^2 + m_x^2\right)H_{ey}\right], \quad (3)$$

$$\frac{\partial m_z}{\partial t} = -\frac{\gamma}{1+\alpha^2}\left[\left(m_x + \alpha m_z m_y\right)H_{ey} - \left(m_y - \alpha m_x m_z\right)H_{ex} - \alpha\left(m_x^2 + m_y^2\right)H_{ez}\right], \quad (4)$$

where $\vec{m} = \vec{M}/M_0$ – the normalized magnetization vector, m_i – its components in the Cartesian coordinate system, M_0 – the saturation magnetization, γ –the gyromagnetic ratio ($\gamma > 0$), α – magnetic dissipation parameter, H_{ei} – the components of the effective field. In the case of the isotropic plate, the components of the effective field included in equations (2-4) have the form:

$$H_{ex} = h_x + H_{0x}, \quad (5)$$

$$H_{ey} = h_y + H_{0y}, \quad (6)$$

$$H_{ez} = H_{0z} - 4\pi M_0 m_z. \quad (7)$$

For the cases of the plate with uniaxial and cubic anisotropy, the components of effective fields have the following form:

$$H_{ex} = h_x + H_{0x} + H_{ax}, \quad (8)$$
$$H_{ey} = h_y + H_{0y} + H_{ay}, \quad (9)$$
$$H_{ez} = H_{0z} - 4\pi M_0 m_z + H_{az}. \quad (10)$$

Let's look at the components of the anisotropy field included in expressions (8-10). For the case of uniaxial anisotropy with angles θ_a , φ_a the expressions for the anisotropy field components have following form (Shavrov and Shcheglov, 2021):

$$H_{ax} = H_{ux} = \frac{2K}{M_0}(-m_x(cos^2\theta_a cos^2\varphi_a + sin^2\varphi_a) + m_y sin^2\theta_a sin\varphi_a cos\varphi_a + m_z sin\theta_a cos\theta_a cos\varphi_a, \quad (11)$$
$$H_{ay} = H_{uy} = \frac{2K}{M_0}(m_x sin^2\theta_a sin\varphi_a cos\varphi_a - m_y(cos^2\theta_a sin^2\varphi_a + cos^2\varphi_a) + m_z sin\theta_a cos\theta_a sin\varphi_a, \quad (12)$$
$$H_{az} = H_{uz} = \frac{2K}{M_0}(m_x sin\theta_a cos\theta_a cos\varphi_a + m_y sin\theta_a cos\theta_a sin\varphi_a - m_z sin^2\theta_a), \quad (13)$$

where K – the uniaxial anisotropy constant.

In the case of the cubic anisotropy and the orientation [001], the components of the anisotropy field can be written as follows:

$$H_{ax} = H_{ax}^{(001)} = \frac{2K_1}{M_0} m_x({m_y}^2 + {m_z}^2), \quad (14)$$
$$H_{ay} = H_{ay}^{(001)} = \frac{2K_1}{M_0} m_y({m_z}^2 + {m_x}^2), \quad (15)$$
$$H_{az} = H_{az}^{(001)} = \frac{2K_1}{M_0} m_z(m_x^2 + {m_y}^2). \quad (16)$$

In the case of cubic anisotropy and orientation [001], the components of the anisotropy field have the following form:

$$H_{ax} = H_{ax}^{(011)} = \frac{2K_1}{M_0} m_x({m_y}^2 + {m_z}^2), \quad (17)$$
$$H_{ay} = H_{ay}^{(011)} = \frac{2K_1}{M_0} m_y(2m_x^2 + {m_y}^2 - {m_z}^2), \quad (18)$$
$$H_{az} = H_{az}^{(011)} = \frac{2K_1}{M_0} m_z(2m_x^2 - {m_y}^2 + {m_z}^2). \quad (19)$$

The cubic anisotropy fields for orientation [111] look like this:

$$H_{ax} = H_{ax}^{(111)} = \frac{K_1}{M_0}({m_y}^3 + m_x {m_y}^2 - \sqrt{2}{m_x}^2 m_z + \sqrt{2}{m_y}^2 m_z), \quad (20)$$
$$H_{ay} = H_{ay}^{(111)} = \frac{K_1}{M_0}({m_y}^3 + {m_x}^2 m_y + 2\sqrt{2} m_x m_y m_z), \quad (21)$$
$$H_{az} = H_{az}^{(111)} = \frac{K_1}{M_0}(\frac{4}{3}m_z^3 - \frac{\sqrt{2}}{3}m_x^3 + \sqrt{2} m_x {m_y}^2). \quad (22)$$

where K_1 – the first constant of cubic anisotropy.

3 SOLUTION ALGORITHM

Let's consider the algorithm for solving the problem in the Matlab system. The LLG equations system (2-4) is solved by the 4-5 orders Runge-Kutta method into the Matlab package with the accuracy control at each step. Firstly, parameters are entered in the task. The right part of the LLG equations system is designed as the separate function. Next, the numerical solution of the system is implemented. The results of the numerical solution are output in the magnetization precession portraits graphs form $m_x(m_y)$, which are projections of the magnetization phase trajectories.

The content of the main program for the Matlab is shown in Listing 1.

Listing 1: The listing of the main program.

```
close all
clear all

global alf h F1 Hx Hy H0 M0 Ku teta_a
fi_a K1
neq=3;

M0=280/(4*pi);
gamma=1.756e7;
H0=252;
alf=0.3;
h=3;
F1=1e8/(gamma*M0);
Hx=0.1*0;
Hy=0;
Ku=0;
teta_a=10*pi/180;
fi_a=0;
K1=8;

for i=1:neq
abt(i)=5e-6;
end;
 teta0=acos(H0/(4*pi*M0));
ink(1)=sin(teta0);
ink(2)=0;
ink(3)=cos(teta0);

tras=1000;
```

```
options = odeset('RelTol',5e-
6,'AbsTol',abt);
[T,Y] = ode45(@y_m2022_2,[0
tras],ink,options);

Nt=length(T);
T1=T(round(Nt/2):Nt);
mx1=Y(round(Nt/2):Nt,1);
my1=Y(round(Nt/2):Nt,2);
figure(1)
plot(mx1,my1,'LineWidth', 2);
set(gca,'FontSize',36,'LineWidth', 4);
xlabel('m_x','FontSize',48);
ylabel('m_y','FontSize',48);
```

Let's describe the text of the main program. First of all, the global parameters are set. The `alf` – the magnetic dissipation parameter, `h` – the alternating field amplitude, `F1` – the alternating field frequency, `Hx, Hy` – components of the weak DC field applied in the plate plane, `H0` – the main DC magnetizing field applied along the normal from the plate plane, `M0` – the saturation magnetization of the plate, `Ku` – the uniaxial anisotropy constant, `teta_a, fi_a` – angles θ_a, φ_a, `K1` – the first constant of the cubic anisotropy. Next, the program introduces the parameter `neq=3` corresponding to the number of differential equations in the system and the values of the listed system parameters. The absolute accuracy is introduced in the for loop for the 3 components of magnetization corresponding to the variables `abt(i)=5e-6` for the system of differential equations LLG solution. `teta0` is the deviation angle of the magnetization from the normal to the plate plane, which is calculated by the formula taken from work (Vlasov et al., 2011). The initial values of the unit magnetization vector components `ink(1), ink(2), ink(3)` are calculated by using this angle. `tras=1000` is the final time for the dynamics of magnetization calculation (in relative units). The set of parameters `options` gives the relative and absolute accuracy of the solution of the LLG system. The `ode45` function implements the solution of the LLG system by the Runge-Kutta 4-5 orders method. After the numerical solution of the LLG equations system, the arrays `mx1, my1` are determined in the program. The steady-state values of the magnetization components m_x, m_y are written in the arrays. The `plot` function implements the plotting of the magnetization precession portrait.

The right part of the differential equations system is described as the separate function in the Matlab system. 2 different functions are introduced to describe the right side of the LLG system for all three cases of the anisotropy. The function corresponding the LLG system for the case of the isotropic plate and the case of uniaxial anisotropy (case 1) is shown in Listing 2.

Listing 2: The LLG system function. Case 1.

```
function f=y_m2022_1(t,m)
 global alf h F1 Hx Hy H0 M0 Ku teta_a
fi_a K1

cg=-1/(1+alf*alf);
neq=3;

f=zeros(neq,1);

mx=m(1);
my=m(2);
mz=m(3);

Heu_x=2*Ku/M0*(-
mx*(cos(teta_a)^2*cos(fi_a)^2+sin(fi_a)
^2)+...
my*sin(teta_a)^2*sin(fi_a)*cos(fi_a)+
mz*sin(teta_a)*cos(teta_a)*cos(fi_a));

Heu_y=2*Ku/M0*(mx*sin(teta_a)^2*sin(fi_
a)*cos(fi_a)-...
my*(cos(teta_a)^2*sin(fi_a)^2+cos(fi_a)
^2)+mz*sin(teta_a)*cos(teta_a)*sin(fi_a
));

Heu_z=2*Ku/M0*(mx*sin(teta_a)*cos(teta_
a)*cos(fi_a)+...
my*sin(teta_a)*cos(teta_a)*sin(fi_a)-
mz*sin(teta_a)^2);

hx=(h*sin(2*pi*F1*t)+Hx+Heu_x)/M0;
hy=(-h*cos(2*pi*F1*t)+Hy+Heu_y)/M0;
hz=(H0-4*pi*mz*M0+Heu_z)/M0;

fx=my*hz-mz*hy;
fy=mz*hx-mx*hz;
fz=mx*hy-my*hx;
fhx=my*fz-mz*fy;
fhy=mz*fx-mx*fz;
fhz=mx*fy-my*fx;
      f(1)=cg*(fx + alf*fhx);
      f(2) = cg*(fy + alf*fhy);
      f(3)= cg*(fz + alf*fhz);
 end
```

The function implements the assignment of the right side of the LLG system (2-4) in the case of the isotropic plate or the uniaxial anisotropy. Moreover, the solution of the system is carried out in relative units: time is normalized by the value $1/(\gamma M_0)$, the alternating field frequency is normalized by the value γM_0 (in the main program).

The function of the LLG system for the case of the cubic anisotropy plate (case 2) is given in Listing 3.

Listing 3: The LLG system function. Case 2.

```
function f=y_m2022_2(t,m)
…
a_orient = '111';
switch a_orient
    case '001'
        Ha_x=2*K1/M0*mx*(my^2+mz^2);
        Ha_y=2*K1/M0*my*(mz^2+mx^2);
        Ha_z=2*K1/M0*mz*(mx^2+my^2);
    case '011'
        Ha_x=2*K1/M0*mx*(my^2+mz^2);
        Ha_y=2*K1/M0*my*(2*mx^2+my^2-
mz^2);
        Ha_z=2*K1/M0*mz*(2*mx^2-
my^2+mz^2);
     case '111'
        Ha_x=2*K1/M0*(mx^3+mx*my^2-
sqrt(2)*mx^2*mz+sqrt(2)*my^2*mz);
Ha_y=2*K1/M0*(my^3+mx^2*my+2*sqrt(2)*mx
*my*mz);
        Ha_z=2*K1/M0*(4/3*mz^3-
sqrt(2)/3*mx^3+sqrt(2)*mx*my^2);
end
hx=(h*sin(2*pi*F1*t)+Hx+Ha_x)/M0;
hy=(-h*cos(2*pi*F1*t)+Hy+Ha_y)/M0;
hz=(H0-4*pi*mz*M0+Ha_z)/M0;
…
```

The listing is given from the end of the line `mz=m(3)` to the definition of the variable `fx`. The fragments of the `function y_m2022_2(t,m)` before the end of the line `mz=m(3)` and after determining the variable `fx`, completely repeat the listing of the previous function `function y_m2022_1(t,m)`. To separate the different cases of orientation of the crystallographic cell the text variable `a_orient` is introduced, for which one of 3 values must be set: `'001', '011', '111'`.

4 RESULTS OF NUMERICAL SOLUTION OF THE LLG SYSTEM

Let's have a look at the main results of the numerical solution of the LLG system obtained using the described calculation program. The plots of all 3 cases of the solution (1. Isotropic plate; 2. Plate with uniaxial anisotropy; 3. Plate with cubic anisotropy) are shown in Figure 2. The values of the parameters given in Listing 1 are used for constructing calculations Figure 2. The parameters are given in the CGS system of units. The frequency of the alternating field is F=100 MHz and corresponds to the variable `F1`. This value is divided by the value `gamma*M0` due to the transition to the relative times and frequencies in the program text.

Let's consider the features of precession portraits in Figure 2. In the case of the symmetric DC field and the isotropic plate, small rings uniformly fill the precession portrait along the generatrix of the large circle. Such precessional portrait is shown in Figure 2a. The presence of the rings accumulations and sparsities on the precessional portrait is visible in the other sub-drawings. The mechanism of formation of the ring accumulations and sparsities was described in works (Shavrov and Shcheglov, 2021; Vlasov et al., 2011; Vlasov et al., 2012; Vlasov et al., 2013) on the basis of energy and vector models.

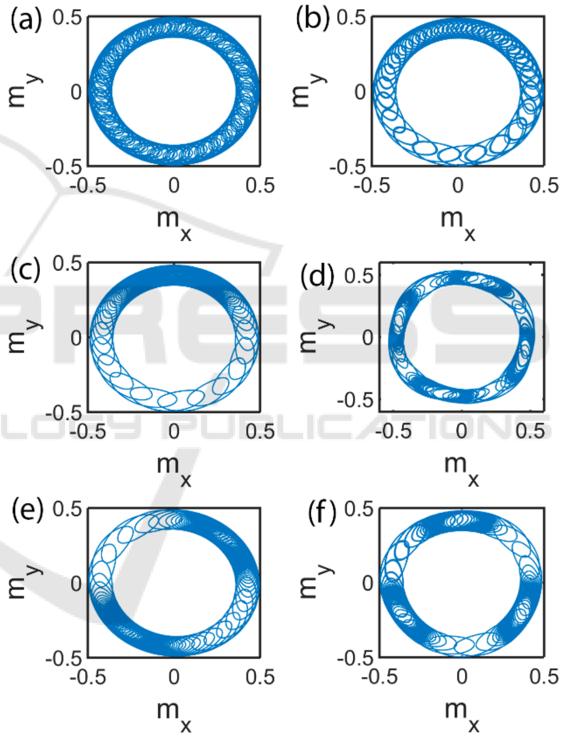

Figure 2: Precession portraits of magnetization for different cases of the anisotropy: (a) the isotropic plate with the symmetric DC field; (b) the isotropic plate with the weak asymmetric field applied along x-axis; (c) the case of the uniaxial anisotropy; (d) the cubic anisotropy with the orientation [001]; (e) the cubic anisotropy with the orientation [011]; (f) the cubic anisotropy with the orientation [111].

The ring accumulations occur at the angle of 90 degrees to the weak DC field applied in the plane for the isotropic plate. The such case is shown in Figure 2b. The additional weak DC field is directed along the x axis and equal to H_{0x}=0.1 Oe. Therefore, the rings accumulation in this portrait is located at the angle of 90 degrees with respect to the x axis and counterclockwise rotated. The polar and azimuthal angles that correspond to the orientation of the easy axis are $\theta_a = 10°$, $\varphi_a = 0$ for the case of uniaxial anisotropy (Figure 2c). Thus the projection of the anisotropy axis onto the plate plane is parallel to the x coordinate axis. The axis is 10° angle with the normal from the plate. The similar rings accumulations and sparsities are observed in Figure 2c, as in the case of the asymmetric DC field (Figure 2b) directed along the x axis. The number of ring accumulations and sparsities depends on the number of minima and maxima of the anisotropy energy in the projection onto the plate plane for the case of cubic anisotropy (Figure 2d, e, f). Figure 2d is constructed for orientation [001]. The value of the cubic anisotropy constant is K_1=160 erg/cm^3. 4 ring accumulations are visible in Figure 2d. The accumulations correspond to the presence of 4 minima and maxima along the precession forming the large circle. Figure 2e is constructed for orientation [011]. The value of the cubic anisotropy constant is K_1=5 erg/cm^3. 2 ring accumulations are visible in Fig. 2e corresponding to 2 minima and maxima along the generatrix of the large circle. Figure 2f is constructed for orientation [111]. The value of the cubic anisotropy constant K_1=8 erg/cm^3. 3 thickenings are visible in Figure 2f, corresponding to 3 minima and maxima along the generatrix of the large circle.

5 CONCLUSIONS

The calculation computer program has been developed in the Matlab system. The computer simulation of the equilibrium position precession in the ferrite plate has been carried out in 3 cases. The first case is the isotropic plate, the second case is the plate with uniaxial anisotropy, the third case is the plate with cubic anisotropy. The listing of the calculation program text is given. The program consists of the main module and two auxiliary functions to describe the right-hand side of the Landau-Lifshitz-Gilbert system of differential equations. The explanations for the features of the obtained magnetization precession portraits based on the presence of maxima and minima of anisotropy energy along the large precession circle are given.

ACKNOWLEDGEMENTS

This work has been supported by the Russian Science Foundation, project no. 21-72-20048.

REFERENCES

Vlasov, V. S., Makarov, P. A., Shavrov, V. G. and Shcheglov, V. I. (2022). Impact excitation of magnetic oscillations by an elastic displacement pulse. *Journal of Communications Technology and Electronics*, 67(7): 876–881.

Vlasov, V. S., Lomonosov, A. M., Golov, A. V., Kotov, L. N., Besse, V., Alekhin, A., Kuzmin, D. A., Bychkov, I. V. and Temnov, V. V. (2020). Magnetization switching in bistable nanomagnets by picosecond pulses of surface acoustic waves. *Phys. Rev. B*, 101(2): 024425.

Shelukhin, L. A., Gareev, R. R., Zbarsky, V., Walowski, J., Münzenberg, M., Pertsev, N. A. and Kalashnikova, A. M. (2022). Spin reorientation transition in CoFeB/MgO/CoFeB tunnel junction enabled by ultrafast laser-induced suppression of perpendicular magnetic anisotropy. *Nanoscale*, 14: 8153-8162.

Barman, A., Mondal, S., Sahoo, S. and De, A. (2020). Magnetization dynamics of nanoscale magnetic materials: a perspective. *J. Appl. Phys.* 128: 170901.

Shavrov, V. G. and Shcheglov, V. I. (2021). *Ferromagnetic resonance in orientational transition conditions*, CRC Press. Boca Raton, 1st edition.

Vlasov, V. S., Kotov, L. N., Shavrov, V. G., and Shcheglov, V. I. (2011). Forced nonlinear precession of the magnetization vector under the conditions of an orientation transition. *Journal of Communications Technology and Electronics*, 56(1): 73–84.

Vlasov, V. S., Kotov, L. N., Shavrov, V. G., and Shcheglov, V. I. (2012). Asymmetric excitation of the two-order magnetization precession under orientational transition conditions. *Journal of Communications Technology and Electronics*, 57(5): 453–467.

Vlasov, V. S., Kirushev, M. S., Kotov, L. N., Shavrov, V. G., and Shcheglov, V. I. (2013). The second-order magnetization precession in an anisotropic medium. Part 2: The cubic anisotropy. *Journal of Communications Technology and Electronics*, 58(9): 847–862.